

1  
2  
3  
4  
5  
6  
7  
8  
9  
10  
11  
12  
13  
14  
15  
16  
17  
18  
19  
20

## Supporting Information

### Preparation and Application of Piperidinium-Functionalized Cross-Linked Polynorbornene-Based Anion-Exchange Membranes

Haixia Zhang,<sup>a,b,†</sup> Yubing Xiao,<sup>a,b,†</sup> Hesong Guo,<sup>c</sup> Xiang Li,<sup>c</sup> Yu Wang,<sup>a,\*</sup> and Wei You<sup>a,b,\*</sup>

<sup>[a]</sup> Beijing National Laboratory for Molecular Sciences (BNLMS), CAS Key Laboratory of Engineering Plastics, Institute of Chemistry, Chinese Academy of Sciences, Beijing, 100190, China

<sup>[b]</sup> University of Chinese Academy of Sciences, Beijing 100049, China.

<sup>[c]</sup> Beijing Cleanway Technology Co., Ltd., Beijing 102611, China.

#### Corresponding Authors

\* Wei You: Email: weiyou@iccas.ac.cn

\* Yu Wang: Email: ywang507@iccas.ac.cn

† These authors contributed equally to this work.

## 21 **Characterization**

22 Fourier transform infrared (FT-IR) spectra were recorded on a Thermo Fisher Nicolet  
23 6700 FT-IR spectrometer. The measurement was carried out in the range of 4000–650  
24  $\text{cm}^{-1}$  with the number of scans per spectrum of 32 and the spectrum resolution of 4  $\text{cm}^{-1}$ .  
25 Scanning electron microscopy (SEM) imaging (Hitachi S-8020) was performed to  
26 observe the morphology. Simplicity<sup>®</sup>UV was used to afford the ultrapure water (18.2  
27  $\text{M}\Omega/\text{cm}^2$  at 25 °C).

28

### 29 **D-2 Copolymer Synthesis.**

30 The copolymerization was performed in a  $\text{N}_2$ -filled glovebox.  $\text{Pd}_2(\text{dba})_3$  (6.9 mg,  
31 0.0075 mmol),  $\text{PCy}_3$  (8.4 mg, 0.030 mmol), and LiFABA (22.8 mg, 0.030 mmol) were  
32 mixed in toluene (3.0 mL) and stirred for 1 h to obtain the activated catalyst solution.  
33 BrNB (2.0 mmol) and DCPD (1.0 mmol) were mixed in toluene (3.0 mL) to obtain the  
34 monomer solution. Then, the activated catalyst solution was filtered and injected into  
35 the monomer solution and the polymerization was carried out at room temperature for  
36 over 12 h. Lastly, the solution was precipitated in methanol and collected by filtration  
37 to obtain the copolymer (D-2) in 95 % yield.

38

### 39 **Cryo-ultramicrotoming and transmission electron microscope (TEM) observation.**

40 The morphology of the D-2-Pip AEM was characterized by transmission electron  
41 microscopy (TEM). Ultrathin sections (<100 nm) were prepared by cryo-  
42 ultramicrotomy at  $-60$  °C using a Leica EM UC6 ultramicrotome and mounted on  
43 copper grids. Imaging was performed on a Hitachi HT7700 TEM operated at 100 kV.

44

### 45 **DSC**

46 Melting ( $T_m$ ) and glass transition ( $T_g$ ) temperatures of the studied membranes were  
47 determined by using a TA Q200 differential scanning calorimetry (DSC) under a  
48 nitrogen atmosphere. The samples were heated under the nitrogen atmosphere from

49 20 °C to 200 °C, and then cooled to –50 °C, followed by heating to 200 °C. All the  
50 heating/cooling rate are 10 °C per minute.

51

## 52 TGA

53 The thermal stabilities of studied membranes were compared by using a TGA 8000  
54 (PerkinElemer) from 50 °C to 750 °C under a nitrogen atmosphere (20 °C /min).

55

## 56 Ion exchange capacity (IEC):

57 First, the membranes in the Cl<sup>-</sup> form was prepared by immersing in 1 M NaCl solution  
58 for 24 h, washed with DI water for three times, dried in vacuo at 60 °C for 24h. The  
59 weights of the dried samples were recorded ( $W_{dry}$ , g). Then, the samples were immersed  
60 in 1 M KNO<sub>3</sub> solution for 48 h to replace Cl<sup>-</sup> in aqueous solution. Finally, the Cl<sup>-</sup> in  
61 the solution was titrated use AgNO<sub>3</sub> solution. The concentration and the used volume  
62 of the AgNO<sub>3</sub> solution were recorded as  $C_{AgNO_3}$  (mmol L<sup>-1</sup>) and  $V_{AgNO_3}$  (L), respectively.  
63 The IEC was then calculated according to the following equation as the average of three  
64 samples:

$$65 \quad IEC(\text{mmol Cl}^-/\text{g}) = \frac{C_{AgNO_3} \times V_{AgNO_3}}{W_{dry}}$$

66

## 67 Water uptake (WU) and swelling ratio (SR)

68 The studied membranes were saturated via immersion in DI water for 24 h at 25 °C.  
69 After removing the residual water with tissue paper, the length and weight of the  
70 saturated membrane were quickly recorded ( $L_{wet}$  and  $W_{wet}$ ). The samples were then  
71 dried at 60 °C in vacuo until reaching a constant weight, with the length recorded as  
72  $L_{dry}$  and the weight recorded as  $W_{dry}$ . The water uptake (WU) and swelling ratio (SR)  
73 were calculated according to the following equation as the average of three sample:

$$74 \quad WU = \frac{W_{wet} - W_{dry}}{W_{dry}} \times 100\%$$

$$75 \quad SR = \frac{L_{wet} - L_{dry}}{L_{dry}} \times 100\%$$

76

### 77 **Conductivity in bulk DI water**

78 The in-plane chloride conductivity of the AAEM sample was measured by four-probe  
79 electrochemical impedance spectroscopy (EIS) using an Ivium Vertex.C.EIS  
80 electrochemical workstation. The conductivity cell BT-112 was purchased from  
81 BekkTeck LLC, and a helpful schematic description of a similar experimental setup has  
82 been reported<sup>1</sup>. The membrane samples in the Br<sup>-</sup> form were clamped into the cell and  
83 the cell was completely immersed in bulk DI water at room temperature during the  
84 measurement time. Electrochemical Impedance Spectroscopy (EIS) was performed by  
85 imposing a small sinusoidal (AC signal) voltage, 10 mV, across the membrane sample  
86 at frequencies between 1 MHz and 1 Hz (scanning from high to low frequencies) and  
87 measuring the resultant current response. A Bode plot was used to assess the frequency  
88 range over which the impedance approached a constant and the phase angle approached  
89 zero. In a Nyquist plot of the data, the high frequency intercept on the real impedance  
90 axis was taken to be the resistance of the membrane. The Br<sup>-</sup> conductivity was then  
91 calculated according to the following equation:

$$92 \quad \sigma = \frac{L}{R \times W \times d}$$

93 Where  $L$  represents the distance between two electrodes in the BT-112 Membrane  
94 Conductivity Cell (0.425 cm);  $R$  is the membrane resistance;  $W$  and  $d$  are the width and  
95 thickness of the samples, respectively.

96

### 97 **In situ de-carbonation under humidified conditions**

98 A similar set-up was adopted from the literature to measure "true hydroxide  
99 conductivities" under humidified conditions.<sup>2, 3</sup> The samples in the HCO<sub>3</sub><sup>-</sup> form were  
100 clamped into the abovementioned BT-112 Membrane Conductivity Cell, which was  
101 located in the corresponding Scribner Associates (SAI) and connected with an FD-HG  
102 temperature and humidity controller (Furande Experimental Equipment Co., Ltd.,  
103 Suzhou, China). The HCO<sub>3</sub><sup>-</sup> conductivity was measured for two hours to ensure the  
104 stabilization of the membrane in the temperature and humidity atmosphere. Through

105 the external electrodes, a constant direct current of 200  $\mu\text{A}$  was applied to the membrane  
106 under nitrogen flow (100 mL/min) at 40  $^{\circ}\text{C}$  and relative humidity (RH) of >98%. Every  
107 10 min, the ionic resistance of the membrane was measured using the abovementioned  
108 4-probe EIS technique, and the in-plane conductivity was then calculated using the  
109 equation:

$$110 \quad \sigma = \frac{L}{R \times W \times d}$$

111 Where  $L$  represents the distance between two electrodes in the BT-112 Membrane  
112 Conductivity Cell (0.425 cm);  $R$  is the membrane resistance;  $W$  and  $d$  are the width and  
113 thickness of the samples, respectively.

114 The anion conductivity was continuously measured until conductivity reached a stable  
115 value (<0.1 k $\Omega$  change in resistance of 3 h). The operating temperatures of the testing  
116 cell and the feeding gas were increased to 50  $^{\circ}\text{C}$ , 60  $^{\circ}\text{C}$ , 70  $^{\circ}\text{C}$  and 80  $^{\circ}\text{C}$  while  
117 maintaining RH, and the conductivities were continuously measured.

118

### 119 **Mechanical properties**

120 The tensile tests were performed on an Instron 3365 universal testing machine. D-2-Pip  
121 aqueous AEM was cut into Dumbbell shape (the length and width of the rectangle area  
122 in the Dumbbell bars are 10 mm and 3 mm, respectively), and the thickness was  
123 measured separately before the test. The mechanical properties of the samples were  
124 assessed with a strain rate of 2 mm  $\text{min}^{-1}$ . All the membranes were tested upon 5  
125 duplicates.

126

### 127 **Alkaline stability**

128 The as-prepared membranes were soaked in an aqueous 1 M KOH solution at 80  $^{\circ}\text{C}$ .  
129 Every seven days, the samples were washed with DI water several times to remove the  
130 residual  $\text{K}^{+}$  and  $\text{OH}^{-}$  ions, and then immersed in an aqueous 1 M  $\text{NaHCO}_3$  solution for  
131 24 hours. After washing with DI water,  $\text{HCO}_3^{-}$  conductivities of the samples were  
132 measured according to the abovementioned method, and  $\text{HCO}_3^{-}$  conductivities were  
133 obtained as the average of three samples.

134

### 135 **Dynamic mechanical analysis (DMA)**

136 The measurements were performed on a TA Instruments DMA 800. The D-2-Pip AEM  
137 was cut into strip-shaped samples measuring 20 mm in length, 5 mm in width, and  
138 approximately 130  $\mu\text{m}$  in thickness. The samples were heated from 0  $^{\circ}\text{C}$  to 90  $^{\circ}\text{C}$  at a  
139 rate of 3  $^{\circ}\text{C}/\text{min}$  under the nitrogen atmosphere.

140

### 141 **SAXS**

142 The small angle X-ray diffraction (SAXS) experiments at 21.7  $^{\circ}\text{C}$  /19.9  $^{\circ}\text{C}$  were  
143 conducted on a Xeuss 2.0 SAXS system (Xenocs SA). X-ray radiation with a  
144 wavelength of 1.5418  $\text{\AA}$  was generated with a Cu  $K_{\alpha}$  X-ray source (GeniX3D Cu ULD).  
145 The sample-to-detector distances were 2501 mm for the SAXS experiments,  
146 respectively. The 2-D SAXS patterns were subsequently collected for an image  
147 acquisition time of 1200 s by using a semiconductor detector (Pilatus 300k, DECTRIS)  
148 with a resolution of 487 $\times$ 619 pixels (pixel size of 172 $\times$ 172  $\mu\text{m}^2$ ). Both the obtained  
149 SAXS patterns were corrected for detector noise, air scattering, and sample absorption.  
150 1-D intensity profiles were integrated from the background-corrected 2-D SAXS  
151 patterns.

152

### 153 **Alkaline water electrolysis**

154 The MEA was prepared through the catalyst-coated substrate (CCS) technique. The  
155 anode catalyst was nickel–iron-based electrocatalyst<sup>4</sup>, while the cathode catalyst was  
156 Pt/C and it was dispersed in the presence of CLi-01 ionomer on the carbon paper gas  
157 diffusion layer. A 1 cm  $\times$  1 cm piece of HER catalyst layers and a 1 cm  $\times$  1 cm piece of  
158 OER catalyst layers were used to assemble in a Mainz-01 water electrolyzer cell (Anhui  
159 Mainz Laboratory Equipment Co., Ltd, Hefei, China) with membranes. A SS-  
160 L3010SPD battery test station was purchased from Bufan Electronics Co., Ltd,  
161 Dongguan, China to control the electrolyzer. 0.1 M, 0.5 M or 1 M KOH were studied  
162 for their AEMWE performance by using polarization curves with an applied voltage

163 from 1.3 V to 2.2 V at 60 °C. Moreover, 1 M KOH were studied for their AEMWE  
164 performance by using polarization curves with an applied voltage from 1.3 V to 2.2 V  
165 at 40 °C, 60 °C or 80 °C Long-term durability tests were conducted with a 1 M KOH  
166 aqueous solution at 60 °C, using a galvanic mode of 1 A cm<sup>-2</sup>.

167

#### 168 **XPS**

169 XPS measurements were performed on a VG ESCALAB 250XI spectrometer. The D-  
170 2-Pip AEMs was immersed in 1 M NaHCO<sub>3</sub> solution for 12 h to exchange the Br<sup>-</sup> with  
171 HCO<sub>3</sub><sup>-</sup>, thereby eliminating potential interference from bromine during subsequent  
172 XPS characterization.

173

174

175

176 **Table S1.** The influence of different piperidine concentrations and reaction times on  
 177 conductivity of D-2-pip membranes

	0.5 h	1 h	2 h	4 h	6 h	12 h
$\sigma^{[a]}$ (Br <sup>-</sup> , mS/cm) at 40 °C			N.A.			10.5
$\sigma^{[a]}$ (Br <sup>-</sup> , mS/cm) at 60 °C			N.A.			14.4
$\sigma^{[b]}$ (Br <sup>-</sup> , mS/cm) at 80 °C	10.5	11.6	12.5	12.8	N.A.	16.7

178 [a] The concentration of the 1-methylpiperidine solution used was 30 vol%. [b] The  
 179 concentration of the 1-methylpiperidine solution used was 5 vol%.

180

181

182

183 **Table S2.** Performance comparison between D-2-Pip AEM and other membranes.

	Stress-at-break (MPa)	Strain-at-break (%)	$\sigma$ at 80 °C (OH <sup>-</sup> , mS/cm)
D-2-Pip	9 ± 5.5	38 ± 8.5	138
x-PFTP-DP-C10-10 <sup>5</sup>	86	34	165
FPAP-3 <sup>6</sup>	84	40	148

184

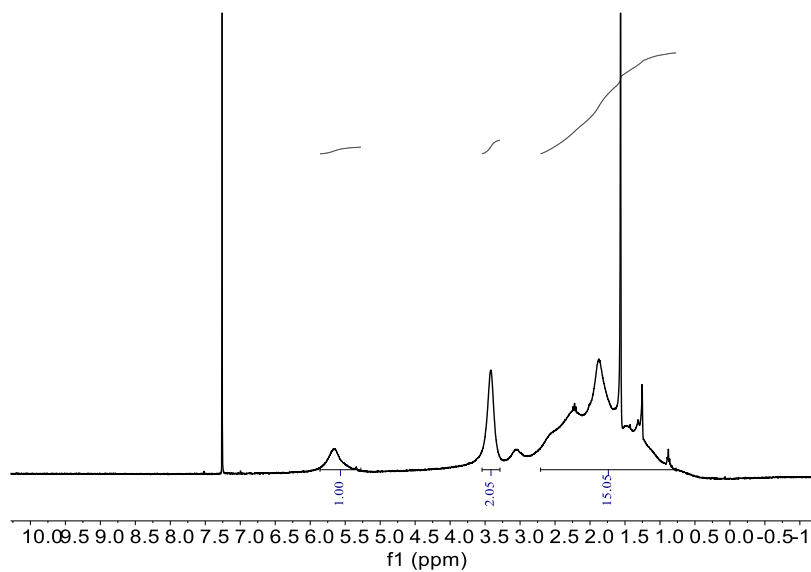
185

186 **Table S3.** The XPS of D-2-Pip AEM

	Br	C	N	O
Atomic/%	0.1	85.49	2.88	11.53

187

188



189

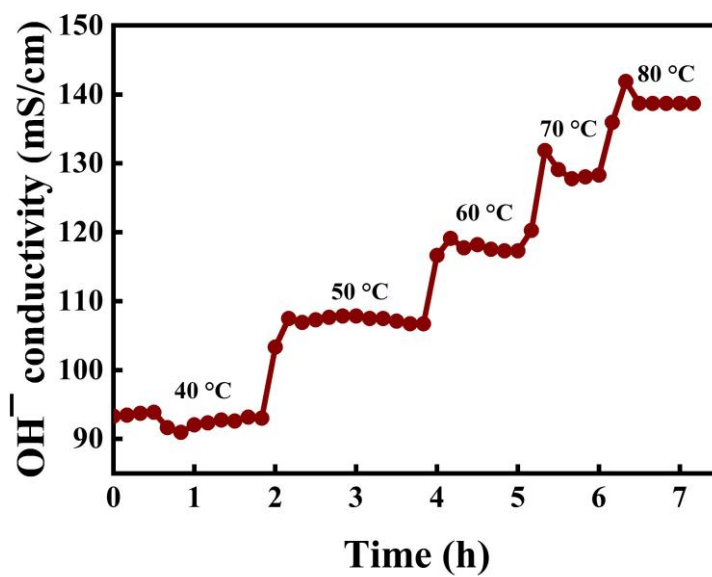
190

191

192

193

**Figure S1.** The  $^1\text{H}$  NMR of **D-2**

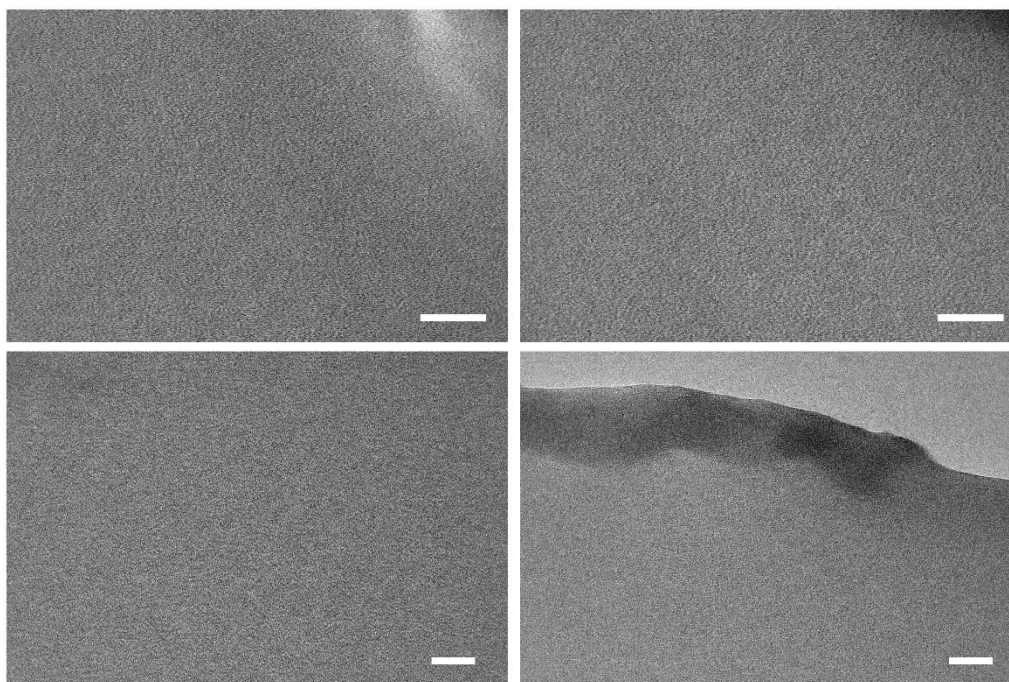


194

195

196

**Figure S2.** Hydroxide conductivities of **D-2-Pip AEM**



197

198 **Figure S3.** TEM images of **D-2-Pip** membranes obtained at different locations. Scale

199

bar represents 50 nm in length.

200

201

202

## 203 **References**

- 204 1. C. H. H. Fujimoto, M. A.; Cornelius, C. J.; Loy, D. A, *Macromolecules*, 2005,  
 205 **38**, 5010-5016.
- 206 2. A. Zhegur-Khais, F. Kubannek, U. Krewer and D. R. Dekel, *Journal of*  
 207 *Membrane Science*, 2020, **612**, 118461.
- 208 3. N. Ziv and D. R. Dekel, *Electrochemistry Communications*, 2018, **88**, 109-113.
- 209 4. Z. C. Li, L. Q. Wang, H. Lee, J. Du, T. Tang, G. H. Ding, R. Ren, W. L. Li, X.  
 210 Cao, S. W. Ding, W. T. Ye, W. X. Yang and L. C. Sun, *Nature Catalysis*, 2024,  
 211 **7**, 944-952.
- 212 5. N. Chen, J. H. Park, C. Hu, H. H. Wang, H. M. Kim, N. Y. Kang and Y. M. Lee,  
 213 *Journal of Materials Chemistry A*, 2022, **10**, 3678-3687.
- 214 6. X. Wu, N. Chen, C. Hu, H. A. Klok, Y. M. Lee and X. Hu, *Adv. Mater.*, 2023,  
 215 **35**, 2210432.

216